To study the role of oxidative stress on Alzheimer's Disease and neurodegeneration using redox sensitive proteins

Nivedita Rangarajan
Indian Institute of Science Education and Research, Pune
Department of Biology

IISER PUNE

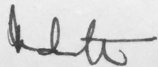Project carried out under the supervision of:

Prof. Vijayalakshmi Ravindranath
Centre for Neuroscience
Indian Institute of Science, Bangalore

And

Prof. L.S. Shashidhara,
Department of Biology
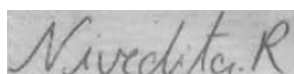Indian Institute of Science Education and Research, Pune

Certificate

This is to certify that this dissertation entitled 'To study the role of oxidative stress on Alzheimer's Disease and neurodegeneration using redox sensitive proteins' towards the partial fulfillment of the BS-MS dual degree programme at the Indian Institute of Science Education and Research, Pune represents the research carried out by Nivedita Rangarajan at the Indian Institute of Science, Bangalore under the supervision of Prof. Vijayalakshmi Ravindranath, Professor, Centre for Neuroscience, during the academic year 2015-2016.

Prof. Vijayalakshmi Ravindranath
Professor, Centre for Neuroscience
Indian Institute of Science, Bangalore

Declaration

I hereby declare that the matter embodied in the report entitled 'To study the role of oxidative stress on Alzheimer's Disease and neurodegeneration using redox sensitive proteins' are the results of the investigations carried out by me at the Centre for Neuroscience, Indian Institute of Science, Bangalore under the supervision of Prof. Vijayalakshmi Ravindranath and the same has not been submitted elsewhere for any other degree.

Nivedita.R

Nivedita Rangarajan

BS-MS Fifth Year Student

Indian Institute of Science Education and Research, Pune

Abstract

Oxidative stress plays an important role in the neuropathology of many progressive neurodegenerative disorders such as Alzheimer's Disease and Parkinson's Disease. An excess of aggregated beta amyloid is one of the major markers of Alzheimer's Disease, and this causes an increase in the oxidative stress. Moreover, in a positive feedback loop, oxidative stress seems to increase the production of beta amyloid as well. Thus, it would be very interesting to be able to study the real-time changes in the redox state of the cell in response to oxidative stress, first in cell lines, and eventually in primary neurons to get a better understanding of the disease. To this end, we performed live-cell imaging experiments on human embryonic kidney cells, and observed an interesting phenomenon upon addition of an external oxidative-stress causing agent (tert-Butyl Hydroperoxide), wherein the oxidative state of the cell seems to come back to normal after an hour or two. This is potentially due to some antioxidant mechanisms present in the cells. This rebound phenomenon was however not observed in Neuroblastoma cells. It remains to be seen how primary neurons will react to oxidative stress, and whether wild type neurons will show a different oxidative state as compared to neurons transgenic for Alzheimer's mutations which might have an intrinsically higher level of oxidative stress due to the presence of excess beta amyloid.

List of Figures

Figure Number	Figure Name	Page Number
Figure 1	Mechanism of roGFP/roTurbo activation	12
Figure 2	Growing up roGFP and roTurbo	18
Figure 3	TBHP end-point experiments using roGFP and roTurbo transfected HEK293 cells	19
Figure 4	Restriction digestion check of lenti-roGFP and lenti-roTurbo clones	21
Figure 5	Transfection check of lenti-roGFP and lenti-roTurbo	21
Figure 6	lenti-roTurbo transduction of primary neurons and HEK293 cells	22
Figure 7	Live imaging with 750uM TBHP treatment	23
Figure 8	Live imaging with 500uM TBHP treatment	24
Figure 9	Live imaging with 250uM TBHP treatment (single replicate)	25
Figure 10	Live imaging with 250uM TBHP treatment (three replicates)	26

Acknowledgements

First and foremost, I would like to thank Prof. Vijayalakshmi Ravindranath for providing me with valuable advice and guidance throughout my project regarding what direction I should take the project and what questions would be most valuable to address. I am grateful to her for letting me work in her lab and learn the fascinating techniques of molecular neuroscience. She also gave me some truly wonderful advice regarding women in science, and set a great example for me as a woman scientist herself, and I will take that with me for the rest of my career.

Next, I would like to thank Aditi Verma from the lab, for helping me from my very first day on the job. She taught me each technique I needed to know with infinite patience, and helped me at each hurdle- be it a failed experiment, designing and planning ahead for a complex experiment, or figuring out the root cause of a persistent cell culture contamination. My project would really have been nowhere without her. I would also like to thank Debajyoti Das for giving me great advice about where I should take my project, and Dr. Reddy for teaching me the nuances and consequences of every step of each technique I utilized. The rest of the lab members- Dr. Ajit, Ruturaj, Sunny, Arathy, Dr. Khader and others were also really helpful throughout my time in the lab, and also gave me sound advice during lab meetings and helped me troubleshoot my experiments.

Finally, I would like to thank my parents and friends for providing me with unending support and helping me keep calm and maintain some balance between finishing my thesis and applying for graduate school.

Introduction

Oxidative stress is caused by a homeostatic imbalance between pro- and anti-oxidant levels, which leads to the generation of reactive oxygen species (ROS) such as H_2O_2, superoxide and hydroxyl radicals, as well as reactive nitrogen species (RNS) such as molecules derived from nitric oxide (Barnham et al., 2004). Although ROS and RNS are beneficial to the system as they are involved in numerous processes like the electron transport chain, signal transduction, kinase activity, gene transcription, angiogenesis, etc. (Uttara et al., 2009, McCord, 2000), their overproduction leads to numerous issues such as DNA, protein and tissue damage, enzyme impairment and an eventual trigger of the apoptotic cascade. Oxidative stress has been implicated in numerous neurodegenerative diseases such as Alzheimer's Disease (AD) and Parkinson's Disease (PD) owing to the susceptibility of some neurons to oxidative damage. Thus it would be interesting to study the role of oxidative stress in neurodegenerative diseases, especially using an approach which would allow the monitoring of the real-time effects of oxidative stress on cells.

Generation of ROS

In order to understand the effects of oxidative stress, we first need to understand how ROS is generated. The source of ROS can either be endogenous or exogenous, and the generation of ROS at either of these sources can be through either direct or indirect interactions (Valko et al. 2006).

Endogenous sources of ROS through cellular metabolism are mitochondria (Loschen et al., 1971), peroxisomes, metabolism of cytochrome P450, etc. (Inoue et al., 2003). In the mitochondria, oxygen produced at the end of the electron transport chain combines with electrons that leak out (even under normal conditions) to become a superoxide (Benzi et al. 1992, Finkel and Holbrook, 2000). A similar mechanism occurs during the hydroxylation reactions in cytochrome P450 (Butler et al., 1993, Valko et al., 2004). Exogenous sources of ROS include exposure to non-genotoxic carcinogens, chlorinated compounds, radiation, etc.

Direct pathways for ROS production include the Fenton reaction (Lloyd et al., 1997) and the Haber-Weiss reaction. In both these reactions, interactions occur between oxygen species and redox active metals, leading to the production of a hydroxyl radical. Indirect interactions mainly involve metallo-enzyme activation through calcium. Typically, in both cases, oxygen interacts with abnormally regulated copper and iron, and leads to ROS production (Barnham et al., 2004).

Effects of ROS

Unchecked ROS production has many consequences. For instance, all four DNA bases, as well as the deoxyribose backbone can be subject to oxidative damage (Dizdaroglu et al., 2002). Further, oxidative stress has been shown to play a role in carcinogenesis (Valko et al. 2006).

Free radicals can cause damage to proteins as well, either through formation of aggregates via cross-linking and dimerization, or through modifications of peptide bonds in amino acids like proline and lysine (Freeman et al., 1982, Trelstad et al., 1981). For instance, ROS can induce oxidative modifications in unsaturated lipids (a process called lipid peroxidation), which leads to the formation of highly reactive lipid peroxy radicals. These radicals then set off a chain reaction, which leads to the formation of breakdown products such as hydroxynonenal (HNE). HNE causes protein modifications through cross-linking of amino acids such as cystine, histidine, etc. which lead to enzyme impairment. The enzymes that are impaired are usually the ones that counteract excessive ROS production, i.e., the antioxidants such as superoxide dismutase and glutathione reductase, among others (Zhong and Yin, 2015). HNE also activates the apoptotic cascade, thus leading to cell death.

The role of ROS in neurodegenerative disorders

ROS is involved in intracellular calcium signaling dysregulation, which then leads to neuronal cell death. Oxidative stress causes calcium influx from the outside of the cell into the cytoplasm via the cell membrane, and into the endoplasmic reticulum through the endoplasmic/sarcoplasmic reticular channels. This causes the release of apoptogenic mitochondrial inhibitors. In the meanwhile, calcium efflux is inhibited. High levels of ROS cause the activation of the mitochondrial permeability transition pore, which opens a channel between the inner and outer mitochondrial membranes, thus leading to free diffusion through the formed channel and a collapse of the electrochemical gradient. Cytochrome c is released into the cytoplasm, which triggers caspase, which then goes on to initiate the apoptotic cascade. Metabolism in the mitochondria is accelerated, and hence disrupted, further leading to cell death. The calcium influx progresses to the nucleus as well, with gene transcription and nucleases being modulated in the nucleus through regulation of phosphorylation and de-phosphorylation, again leading to apoptosis. (Ermak and Davies, 2001, Emerit et al., 2004). Moreover, dysfunction of the mitochondria can cause excessive activation of glutamate receptors, leading to the accumulation of glutamate (an excitatory neurotransmitter) intracellularly, causing an increase in calcium influx, which eventually leads to cell death.

Alzheimer's Disease (AD)

AD is a progressive neurodegenerative disorder that involves memory loss, motor, and cognitive impairment. It is characterized by neurofibrillary tangles, deposition of aggregated beta amyloid (Aβ) in the cortex and other sub-cortical regions, and the loss of neurons. Alterations are sometimes seen in the cholinergic and noradrenergic systems as well (McKhann et al., 1984). AD can either be hereditary, or sporadic. In AD, the amyloid precursor protein (APP) is sequentially cleaved by secretases, forming an amyloid beta fragment (either 39, 40 or 42 amino acids in length). Aβ fragments can aggregate to form plaques (Goedert and Spillantini, 2006). This is usually followed by abnormal hyperphosphorylation of tau proteins, leading to

neurofibrillary tangles. Further, synaptic failure is common in the hippocampus and other regions (Querfurth and LaFerla, 2010).

The role that oxidative stress plays in AD is that Aβ co-ordinates with copper and iron ions and produces H_2O_2 and lipid peroxides via the Fenton reaction (Behl et al., 1994, Smith et al., 1997). With the accumulation of the peroxides, the apoptotic cascade is eventually activated through mitochondrial dysfunction (Zhao and Zhao, 2013). Furthermore, the effect seems to be cyclical, where an increased level of oxidative stress increases the Aβ production and accumulation as well (Li et al., 2004). ROS is also involved in neuronal cell death through its interaction with Aβ, wherein it mediates the ASK1 activation pathway, eventually leading to cellular apoptosis. Aβ and ROS interact and activate the JNK pathway, which then triggers apoptosis (Kadowaki et al., 2005). Oxidative stress also seems to play a role in the tau pathway, wherein it causes modifications to the cytoskeleton, thus leading to the formation of neurofibrillary tangles (Perry et al., 2002). In the case of hereditary AD, where the apoliprotein E4 allele is inherited, ApoE4 adducts with HNE, and chelates with copper and iron ions as well, indicating a role in oxidative stress (Smith et al., 2000, Miyata and Smith, 1996). The compound tert-Butyl hydroperoxide (TBHP) used in the entirety of this project to induce oxidative stress causes an increase in lipid peroxidation, cytosolic calcium ions, and hence an increase in cytotoxicity as well, thus leading to cell death (Kučera et al., 2014).

Parkinson's Disease

Parkinson's Disease (PD) is another neurodegenerative disorder that leads to motor impairments such as increased muscle tone (rigidity), bradykinesia, etc. and is characterized by the selective loss of neuromelanin-containing dopaminergic neurons in the Substantia Nigra pars compacta (SNpc) and the striatum (Chinta and Andersen, 2008, Damier et al., 1999). Dopaminergic neurons, being more sensitive to oxidative stress, are more vulnerable to cell death.

Dopamine (DA) itself can cause oxidative stress if its metabolism is unchecked. Dopamine usually undergoes auto-oxidation, and forms free radicals and a quinone-modified version of itself- dopamine quinone. However, in PD conditions, dopamine

forms DA quinone and H_2O_2 instead (Dias et al., 2013). DA quinone then modifies proteins such as DJ-1, Parkin, etc., all a part of PD pathology, and leads to their dysfunction. It also modifies alpha-synuclein, another player in PD pathology, and converts it to a cytotoxic form (Conway et al., 2001, Hwang, 2013). Further, DA quinone leads to mitochondrial dysfunction (Lee et al., 2002). All these factors combined lead to cell death. Neuromelanin-containing dopaminergic neurons seem to be especially sensitive to cell death because neuromelanin (for which DA quinone is a pre-cursor) is involved in neurodegeneration and neuroinflammation (Zecca et al., 2008). Thus, ROS plays a significant role in PD as well.

Measuring ROS

Now that we understand that ROS plays a very important role in neurodegenerative disorders, we need to find some means of studying the redox status of cells in real-time. This can be done, by using the proteins roGFP and roTurbo in either live-cell imaging experiments, or end point experiments. Both these proteins are redox sensitive molecules that can give a real-time measure of the oxidative state of a cell. roGFP was first developed in 2004 in order to measure changes in the redox potential of mitochondria and mammalian cells (Hanson et al., 2004, Dooley et al., 2004). roGFP is a modified version of GFP, wherein two surface-exposed cysteines were introduced at positions 147 and 204 on adjacent strands of the beta barrel structure of GFP. The roGFP molecule can fluoresce at two excitation maxima-405nm and 488nm. The ratio of excitation between these two maxima depends on the oxidative state of the cell. When the oxidative state increases, a di-sulphide bridge forms between the two cysteines and protonation is promoted. Thus, the intensity of the peak at 405nm increases, and that at 488nm decreases. This di-sulphide bridge formation is reversible, and when the oxidative state decreases, the bridge breaks, and the peak at 488nm increases at the cost of the one at 405nm (Weirer et al., 2011). A schematic is provided in Figure 1. roGFP and roTurbo are around 750bp long, just like regular GFP.
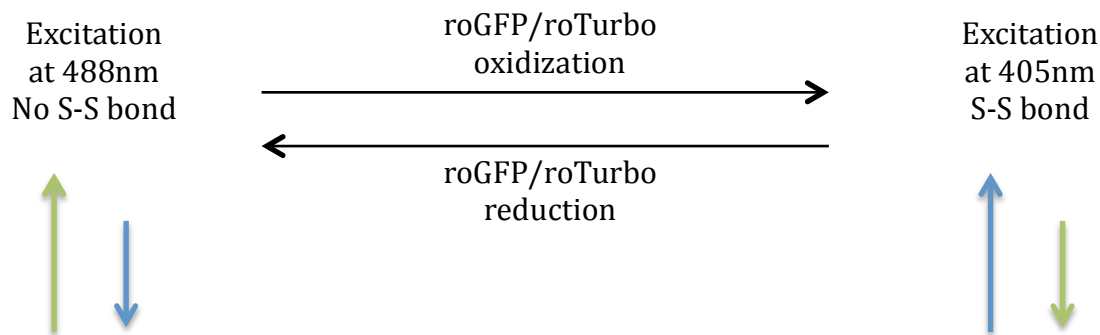
Figure 1: Mechanism of roGFP/roTurbo activation. Schematic of change in intensities at two fluorescent peaks for roGFP and roTurbo depending on oxidative state.

roTurbo is another redox sensitive protein that was developed as an alternative to roGFP, albeit more sensitive (Dooley et al., 2012). This molecule was constructed as a modification of roGFP2, by including six superfolder mutations that enable folding even on poor fusion to peptides (Pedelacq et al., 2006). This increases the brightness of the protein and also enables it to oxidize more readily. However, its mode of operation is the same as roGFP (Fig.1).

In this project, we looked at the role of oxidative stress in neurodegeneration and Alzheimer's Disease by initially monitoring the oxidative state of cell lines using the redox sensitive proteins roGFP or roTurbo in response to a ROS inducing agent-tert-butyl hydroperoxide (TBHP). We saw an increase in oxidative state, as expected, but also saw a curious and as yet unobserved rebound phenomenon in one cell line where the oxidative state of the cells seems to come back to normal within 20 minutes, possibly due to the antioxidant properties of the cell kicking in. We hope to take this further, by looking at the change in the oxidative state of primary neurons from the cortex of wild type and transgenic mice (transgenic for the amyloid precursor protein, hence an AD model), and observing the differences in their response to oxidative stress.

Materials and Methods

The first few months of the project work involved learning the various techniques and setting up the groundwork for the experiments. This included learning bacterial work, cell culture handling and maintenance, imaging with the confocal microscope, and virus generation.

Growing up plasmids

Using an existing sample of pure plasmid (for both roGFP and roTurbo), I performed bacterial transformation in order to obtain pure colonies of bacteria containing the required gene. I inoculated one of the colonies in Luria Broth (LB) overnight, in order to get a large quantity of bacteria with my plasmid. I then performed a maxiprep (Qiagen maxiprep kit) to extract the pure plasmid from the bacterial cells. I tested whether the plasmid obtained was the correct one through two methods- one was restriction digestion, and the other was transfection of N2a (neuroblastoma) cells. A standard restriction digestion was performed. Transfection was done with Lipofectamine and Plus reagents (ThermoFisher Scientific, standard protocol). The fragments obtained upon digestion were as expected, and the cells had been successfully transfected, showing fluorescence at the correct wavelengths of 488nm and 405nm.

End-Point experiments

These experiments were performed on HEK293 cells, which were maintained in a DMEM (Dulbecco's modified Eagle's medium) medium according to the ATCC protocol. I had two sets of cells- one control and the other treated. In the treated cells, I added a particular concentration of TBHP (either 250uM, 500uM, 750uM or 1mM), and incubated the cells for either one or two hours. I then washed the cells with 1x PBS and fixed them using 4% paraformaldehyde (PFA) on slides. I also washed and fixed the control cells simultaneously in an identical manner. I then

imaged both the sets of cells using the Zeiss LSM780 confocal microscope under the 40x oil objective, checking the fluorescence intensity at 488nm and 405nm.

Cloning of roTurbo into p-lenti backbone

In order to generate a virus, I first needed the roTurbo gene to be present in a lentiviral backbone. Thus, I performed a restriction digestion on two plasmids, one containing the roTurbo gene, and the other containing the p-lenti backbone, and digested one side of each of the required fragments (Qiagen elution kit). I then performed end-filling on the staggered ends using 1ul T4 polymerase, 0.5ul dNTP, 5ul 2.1 Buffer for 15 minutes at 12°C. After an isopropanol clean up, I performed another restriction digestion to digest the other end of the fragments as well. This was then run on a gel. The correct fragments (one containing the roTurbo gene only, and the other containing the p-lenti backbone only) were then cut from the gel and eluted (Qiagen gel extraction and elution kit). I then ligated roTurbo into p-lenti using T4 ligase (1ul) and 10x T4 ligase buffer (1ul) overnight at 16°C, with different roTurbo:p-lenti ratios of 5:1, 3:1 and 1:1.

This plasmid now with roTurbo in a lentiviral backbone, was then transformed and grown via a miniprep (Qiagen miniprep kit), and I screened the bacterial colonies obtained to see if they had the correct insert. The screening was done through restriction digestion and a transfection check. Several colonies were obtained with roTurbo in the lentiviral backbone. I took one of these (having a 3:1 roTurbo:p-lenti ratio) and generated a large quantity of it by growing up the plasmid (Qiagen maxiprep kit). The same procedure was also repeated for roGFP, and I obtained roGFP in a lentiviral backbone.

Both these plasmids were then sent for sequencing.

Virus generation

Virus generation also requires two packaging plasmids- pMD2.G and psPAX2. They were grown (Qiagen maxiprep kit) in order to obtain large quantities required for virus generation. These two plasmids, along with lenti-roTurbo were then simultaneously transfected in ten 15cm dishes of HEK293 cells through the calcium phosphate method of transfection. 50ug of lenti-roTurbo was used, along with 25ug of PMD2.G and 25ug of psPAX2. The plasmids dissolved in 225ul $CaCl_2.2H_2O$ and 1.65ml of 0.1x TE, was then bubbled through a solution of 1.875ml 2x HBS and allowed to rest for 25 minutes. This was then added to each of the ten plates. Viral production started in 8 hours, and the media containing the virus was collected at regular intervals over 48 hours. This media was then filtered (through a 0.45um filter) and vacuum centrifuged in order to obtain a pellet containing the virus. This pellet was then re-suspended in media and stored at -80°C in small aliquots for future use. The steps from virus collection onwards must be done at a BSL2 area.

The viral titer was checked using serial dilutions added to different wells containing a roughly fixed number of HEK293 cells. The dilution rate in the well at which around 35-40% of the cells are transduced is noted, and the viral titer is calculated as:

$$x \text{ TU/ul} = ((\% \text{ of cells transduced}) \times (\text{no. of cells plated}))/(\text{amount of virus in the well in ul})$$

where x is the viral titer in terms of TU or transforming units per ul (i.e. active viral particles per ul)

The viral titer was found to be 2.15 x 10^6 TU/ul for roTurbo.

Live imaging

All the live imaging for the project was done on the Zeiss LSM780 confocal microscope under the 40x oil objective. Lasers at 488nm and 405nm were used for imaging. The cells were plated in 4-welled glass bottom dishes and transfected/

transduced with roTurbo within 16 hours. They were then imaged either after 30 hours or 48 hours depending on whether they were transfected or transduced. Live imaging was done in an incubation chamber placed on the stage of the microscope, which maintained the temperature at 37°C and CO_2 levels at 5% (same as the incubator the cells are maintained in). Controls were imaged first for an hour, followed by overnight (12hr) imaging of the cells treated with a particular concentration of TBHP, starting from the minute of TBHP addition. At the end of this, the control cells were measured once again. A z-stack of the cells was taken, such that the entire cell was covered. Each field was imaged every 10-12 minutes on average.

Image analysis

The intensities of the cells were analyzed using the software MetaMorph (Molecular Devices, Inc., Sunnyvale, CA). Regions of interest were drawn around the cells, and the software produced the average intensity for that region (both at 488nm and 405nm) for the maximum intensity projection at every time step. Similarly, the background intensity was also obtained. The ratio of the intensities at the green wavelength (488nm) to the blue wavelength (405nm) was calculated at each time step as follows:

Ratio= (Green intensity-green background)/(Blue intensity-blue background)

The final graphs were either created on Microsoft Excel (2011), or using Matlab (Mathworks 2011).

Limitations and range of validity

There were some limitations in the live imaging and image analysis. After transduction of the cells, it is not easy to image the cells at the exact same time post-transfection/transduction. Thus, the level of roGFP or roTurbo expression won't be

identical. However, this should not matter, as the values being calculated are ratiometric in nature. Also, there is a 1-2 min time lag between the actual addition of TBHP and the start of imaging as there is some portion of the settings that have to be set up.

Due to intracellular variability, low intensity at the blue wavelength and a greater amount of noise in the images at this wavelength, some cells had a negative intensity value on subtracting the background. As this did not make physical sense, these cells were omitted. Furthermore, in the end-point experiments, we will only be able to see the cells that survived the treatment. There might be cells that are sensitive to oxidative stress and show a change in intensity ratio, but die out before the end of the treatment time. This experiment is therefore not going to give us that information.

Results

Growing up roGFP and roTurbo

This project initially started off with learning various techniques in molecular neuroscience. As I was going to work with redox sensing proteins (roGFP and roTurbo), I first had to grow them up and check if they were correctly grown. This check was done through restriction digestion (RD) and transfection (Figure 2).
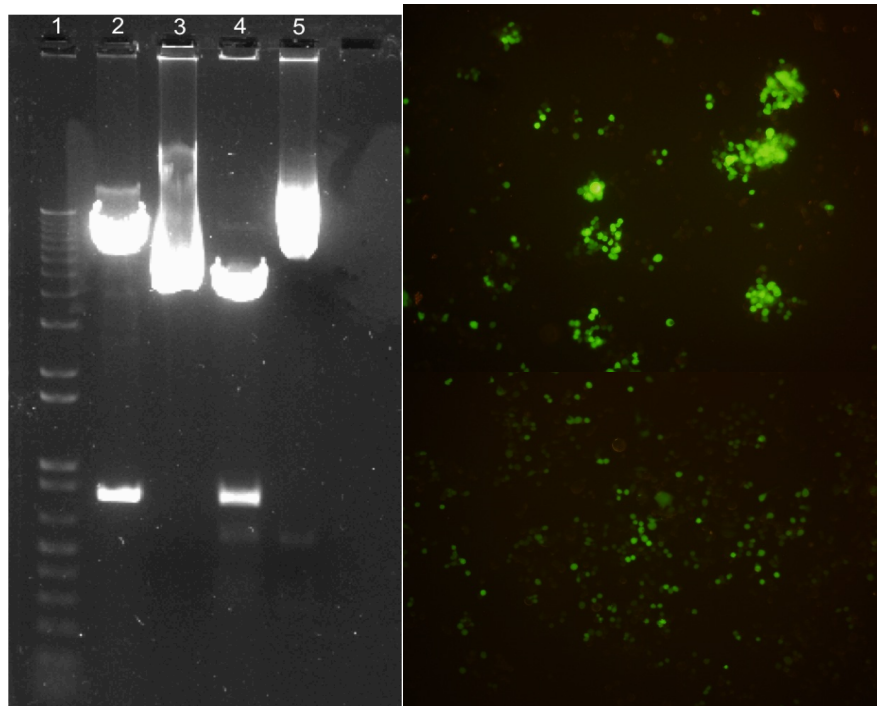

Figure 2: Growing up roGFP and roTurbo. *Left:* Products of restriction digestion. Lane 1- 1Kb Plus reference ladder. Lane 2- roGFP after restriction digestion (RD). Lane 3- roGFP without RD. Lane 4- roTurbo after RD. Lane 5- roTurbo without RD. Note that lanes 2 and 4 have one DNA band at around 750bp, which is roughly the size of roGFP and roTurbo. *Top Right:* roTurbo expression ~30 hours after transfection. *Bottom Right:* roGFP expression ~30 hours after transfection.

End-point experiments using roGFP and roTurbo

As I had obtained the correct plasmids, I now had to determine the range of concentrations of tert-Butyl Hydroperoxide (TBHP) that would produce changes in the oxidative levels of the cells, without causing apoptosis. Thus, I treated different sets of HEK293 cells with 250uM, 500uM, 750uM or 1mM TBHP for an hour, fixed them, and observed the ratio of green to blue intensity for the treated versus the control cells. If the TBHP has indeed caused an increase in the oxidative state of the cells, the intensity at blue should increase and green should decrease (compared to the controls), thus reducing the ratio of green:blue intensity. Thus, the treated cells should have a smaller ratio as compared to the control. The results are seen in Figure 3.
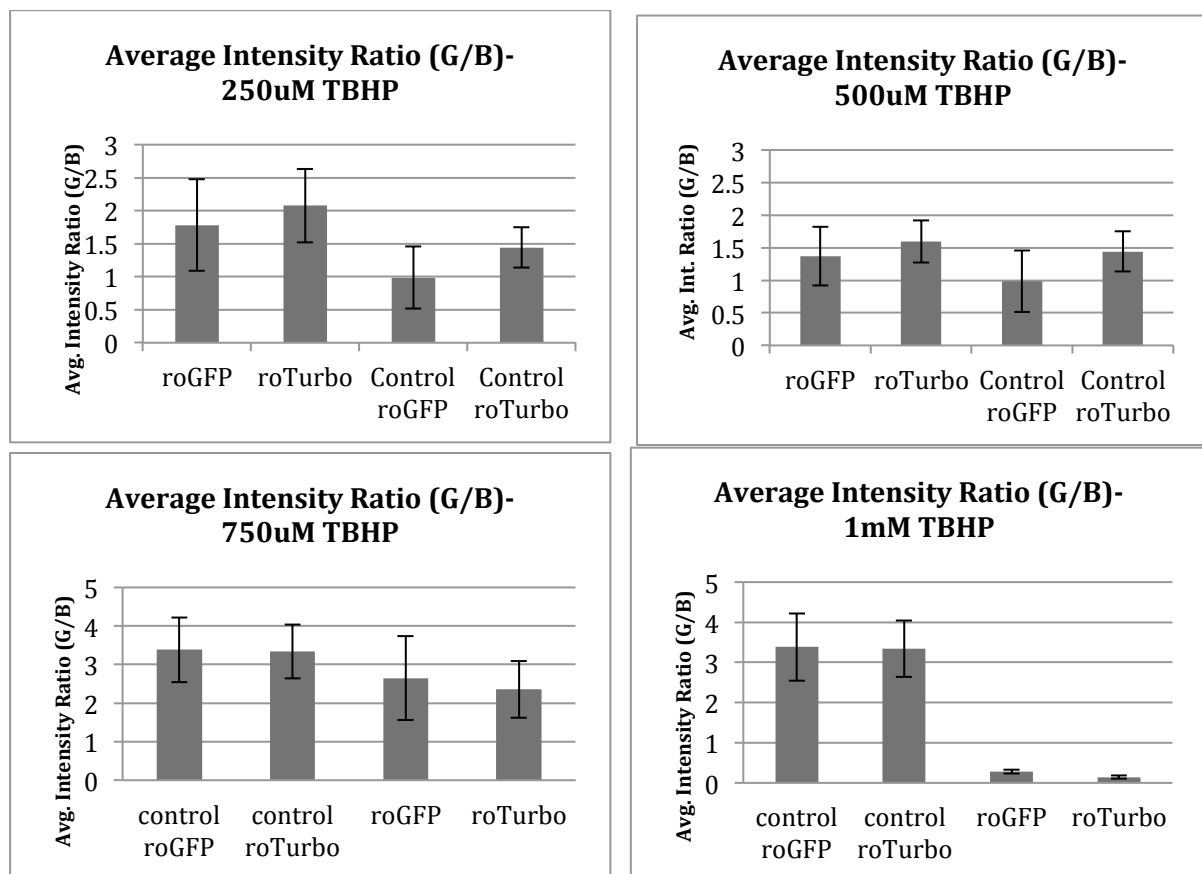

Figure 3: TBHP end-point experiments using roGFP and roTurbo transfected HEK293 cells. n= ~60 cells per treatment per concentration. Error bars represent standard deviation. *Top Left:* Treated vs. control, 250uM TBHP. *Top Right:* Treated

vs. control, 500uM TBHP. *Bottom Left:* Control vs. treated, 750uM TBHP. *Bottom Right:* Control vs. treated, 1mM TBHP.

As can be seen, the ratio in treated as compared to control goes down only in 750uM and 1mM TBHP. This might indicate that only these concentrations of TBHP are effective, but this is not a very nuanced experiment, as we do not know the fate of the cells that might be responding to the treatment, but die out before the end of the hour. Thus, although this experiment gives a rough idea of what concentrations of TBHP to start at, a live-imaging experiment will give a better picture.

Due to persistent contamination of cells while using lipofectamine or calcium phosphate for roGFP/roTurbo transfection, we decided to use a virus to transduce the cells instead. Moreover, a viral roGFP/roTurbo will also be useful in transducing primary neurons in future experiments.

Cloning of roTurbo and roGFP into p-lenti backbone

Since the roTurbo was in another backbone, and needs to be in a lentiviral backbone before it can be packaged as a virus, we needed to clone roTurbo into the p-lenti backbone. Upon screening through numerous colonies having either 1:1, 3:1 or 5:1 ratios of roTurbo:p-lenti concentration prior to ligating, we found some colonies that had a fragment at the correct base pair length of around 750bp (Figure 4). We double-checked this by transfecting the cells (Figure 5), and sending the plasmids for sequencing. The same was repeated for roGFP.

Upon sending the lenti-roGFP and lenti-roTurbo plasmids for sequencing, we confirmed that the sequences of roGFP and roTurbo were in accordance with that described in the literature.
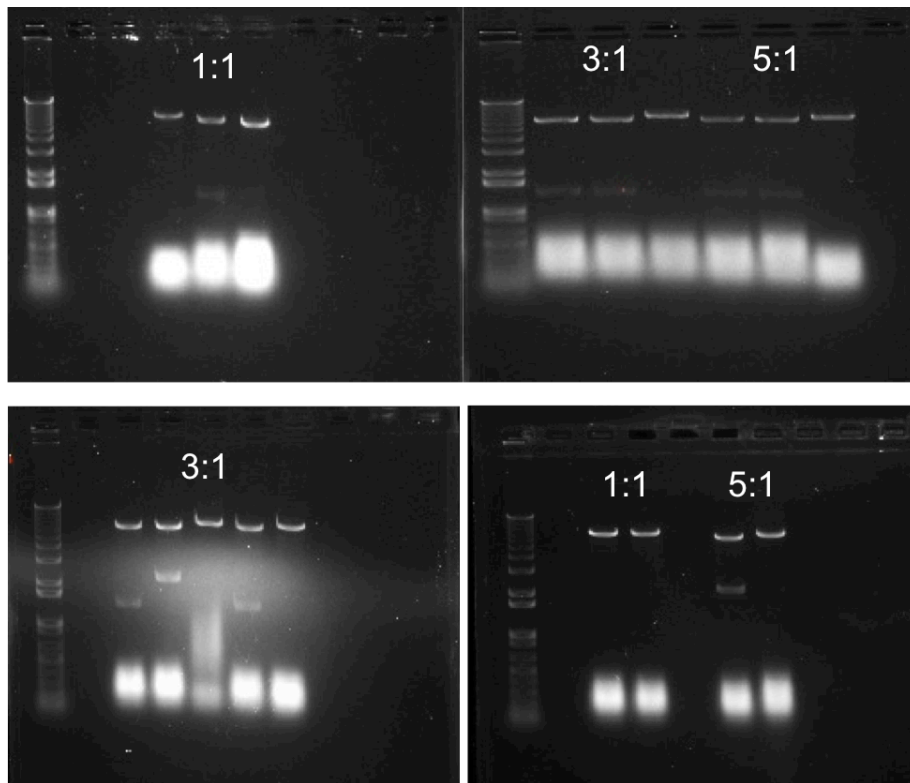
Figure 4: Restriction digestion check of lenti-roGFP and lenti-roTurbo clones. *Top Row:* RD of lenti-roGFP. Five colonies seem to be successful- middle lane 1:1, first two lanes 3:1, first two lanes 5:1, as they have a DNA fragment at around 750bp. *Bottom row:* RD of lenti-roTurbo. Two colonies seem to be successful- first and fourth lane in 3:1, as they have a DNA fragment at around 750bp. (See text for meaning of ratios 1:1, 3:1 and 5:1). First lane in each panel: 1Kb Plus DNA ladder.
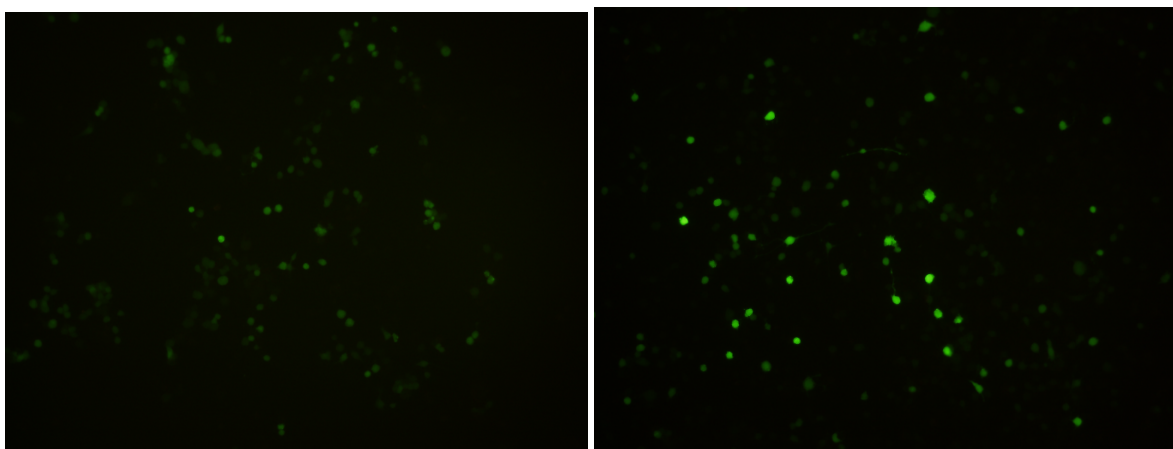

Figure 5: Transfection check of lenti-roGFP and lenti-roTurbo. *Left:* lenti-roGFP transfection. *Right:* lenti-roTurbo transfection.

Virus generation

Since we could not discern whether roGFP or roTurbo was more sensitive for measuring oxidative stress, we decided to proceed with roTurbo for virus production as it had a higher intensity overall. The lenti-roTurbo virus produced finally had a titer of 2.15 x 10^6 TU/ul. We then checked to see if the virus worked by transducing both primary neurons and HEK293 cells (Figure 6).
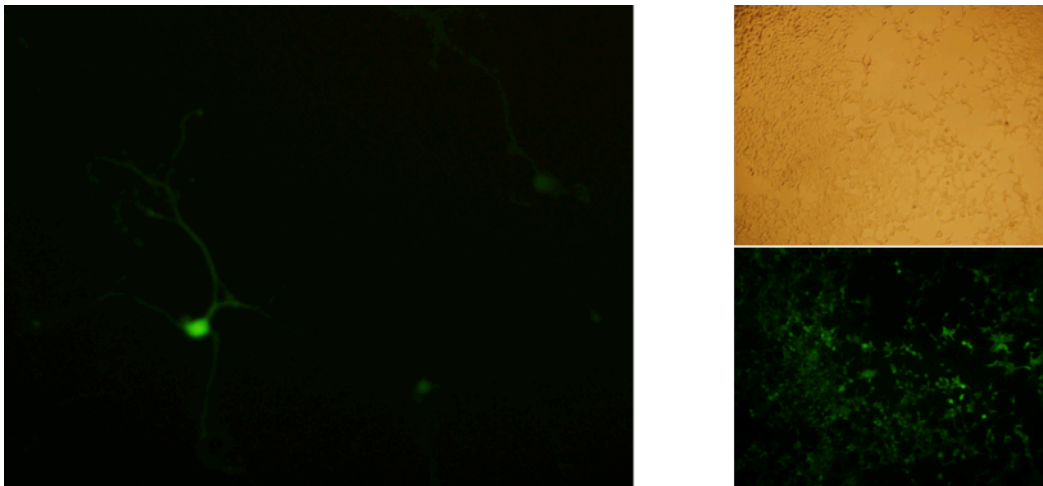

Figure 6: lenti-roTurbo transduction of primary neurons and HEK293 cells. *Left:* Wild type primary cortical neurons transduced by viral roTurbo. *Right Top:* Bright-field image of HEK293 cells transduced by viral roTurbo. *Right Bottom:* Same cells as top, fluorescing.

Live imaging results

As we had established through the end-point experiments that 750uM TBHP was a good place to start for the live-imaging experiment, we performed an overnight live imaging experiment with HEK293 cells (Figure 7 Top Panel). Although at first-glance the cells seem to not have a trend, and have a large intercellular variability, around 30 treated cells showed an interesting trend where the ratio drops rapidly, then starts increasing again (Figure 7 Bottom Panels). The cells had been transduced with lenti-roTurbo 2 days prior to the experiment.
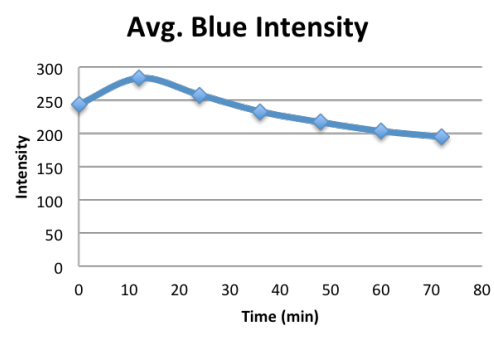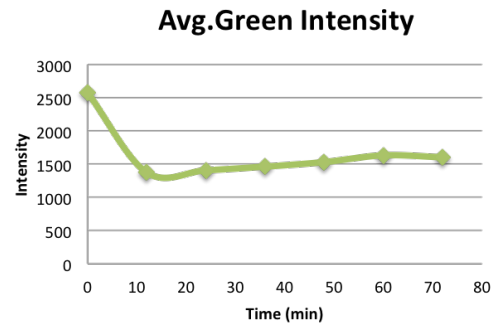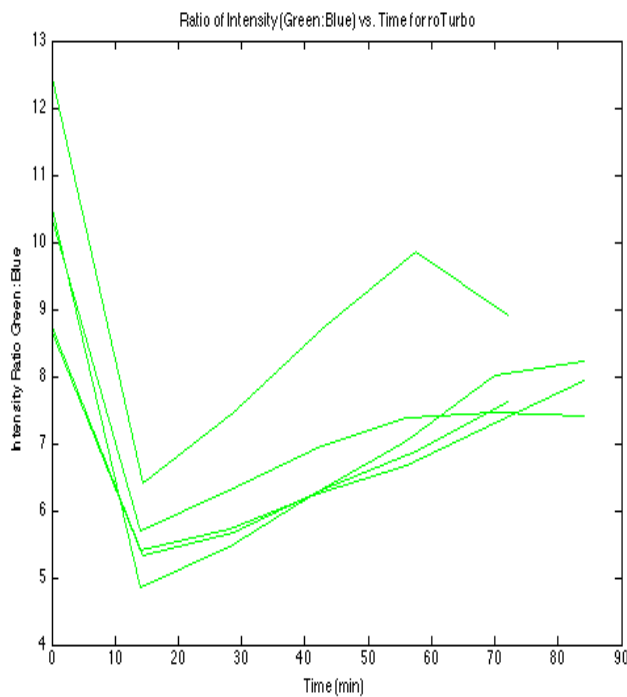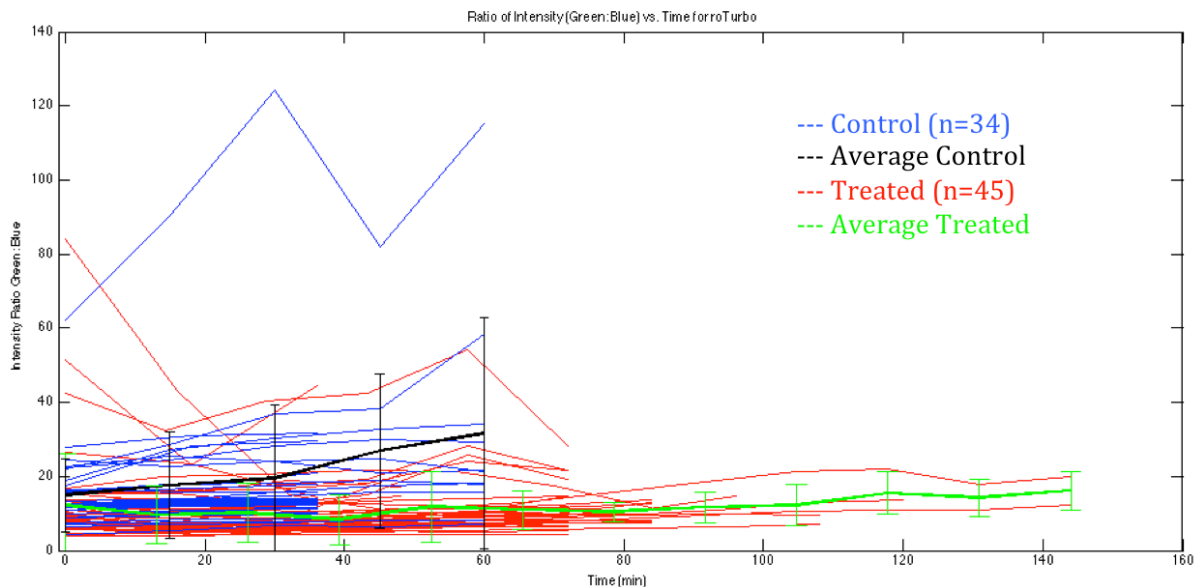
Figure 7: Live imaging with 750uM TBHP treatment. Error bars represent standard error. *Top Panel:* All 34 control HEK293 cells and 45 treated cells for the 750uM TBHP overnight treatment. Control cells imaged only for one hour, treated cells died within 2.5 hours. *Bottom Left Panel:* Change in green:blue intensity ratio over time for 5 representative cells. Bottom *Right Panels:* Separate change in green and blue intensity over time for one representative cell.

Since the drop in the ratio was sharp, we decided to go for a lower concentration of TBHP (500uM) and repeat the experiment (Figure 8).
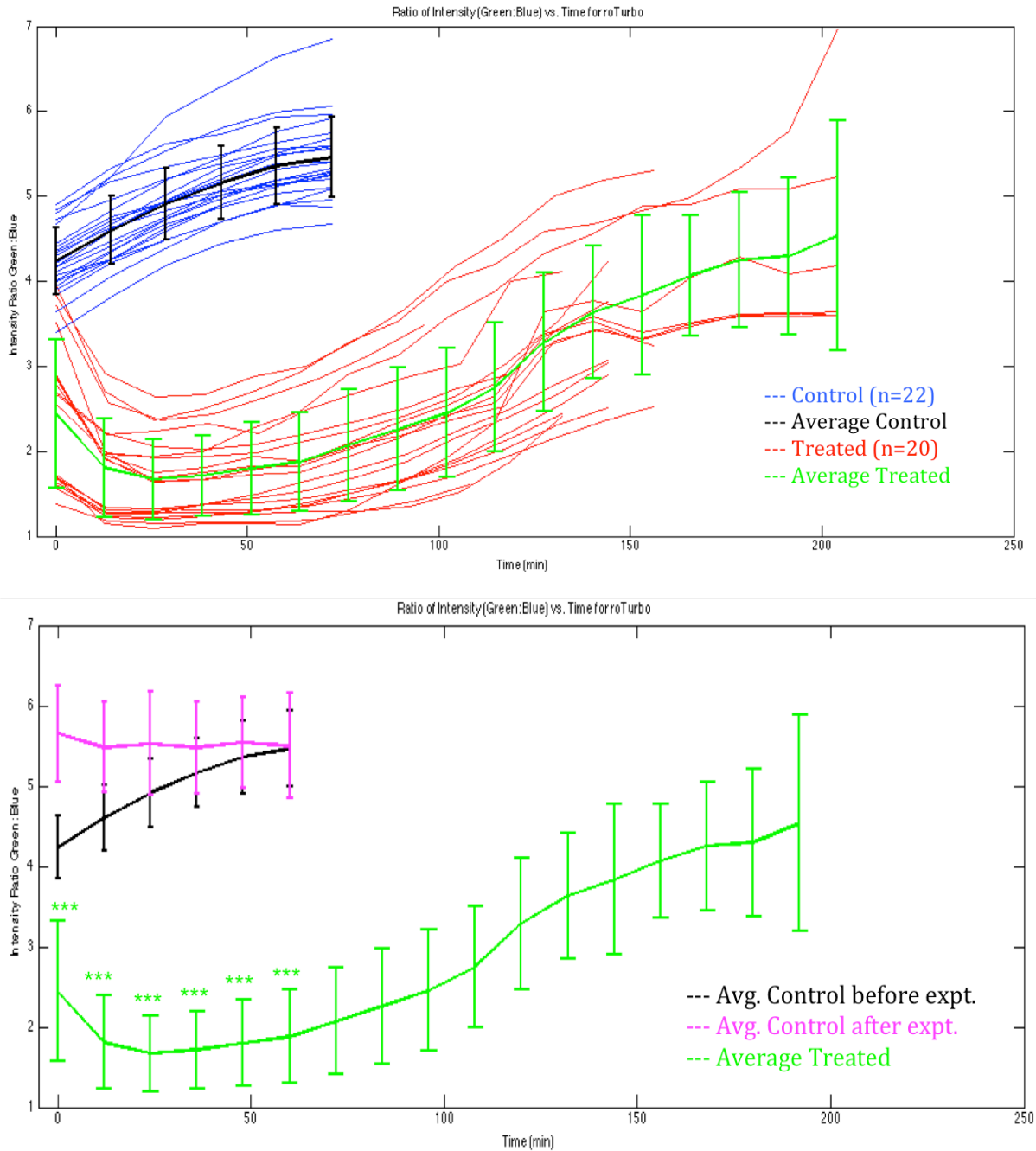
Figure 8: Live imaging with 500uM TBHP treatment. *Top Panel:* All 22 control HEK293 cells and 20 treated HEK293 cells for the 500uM TBHP overnight treatment. Control cells imaged only for one hour, treated cells died within 3.5 hours. *Bottom Panel:* Only the average plot of treated cells and control cells. Black line- control cells imaged prior to the TBHP treatment. Pink line- control cells imaged after the overnight TBHP treatment (averaged over 20 cells). The pink line has been super-imposed starting from 0 minutes instead of at 720 minutes to give a better idea of relative values. All error bars represent standard error.

This treatment was on Human Embryonic Kidney cells, so the same was repeated on a Neuroblastoma (N2a) cell line. As these neurons are more susceptible to oxidative stress, a lesser concentration of TBHP (250uM) was tried (Figure 9, 10).

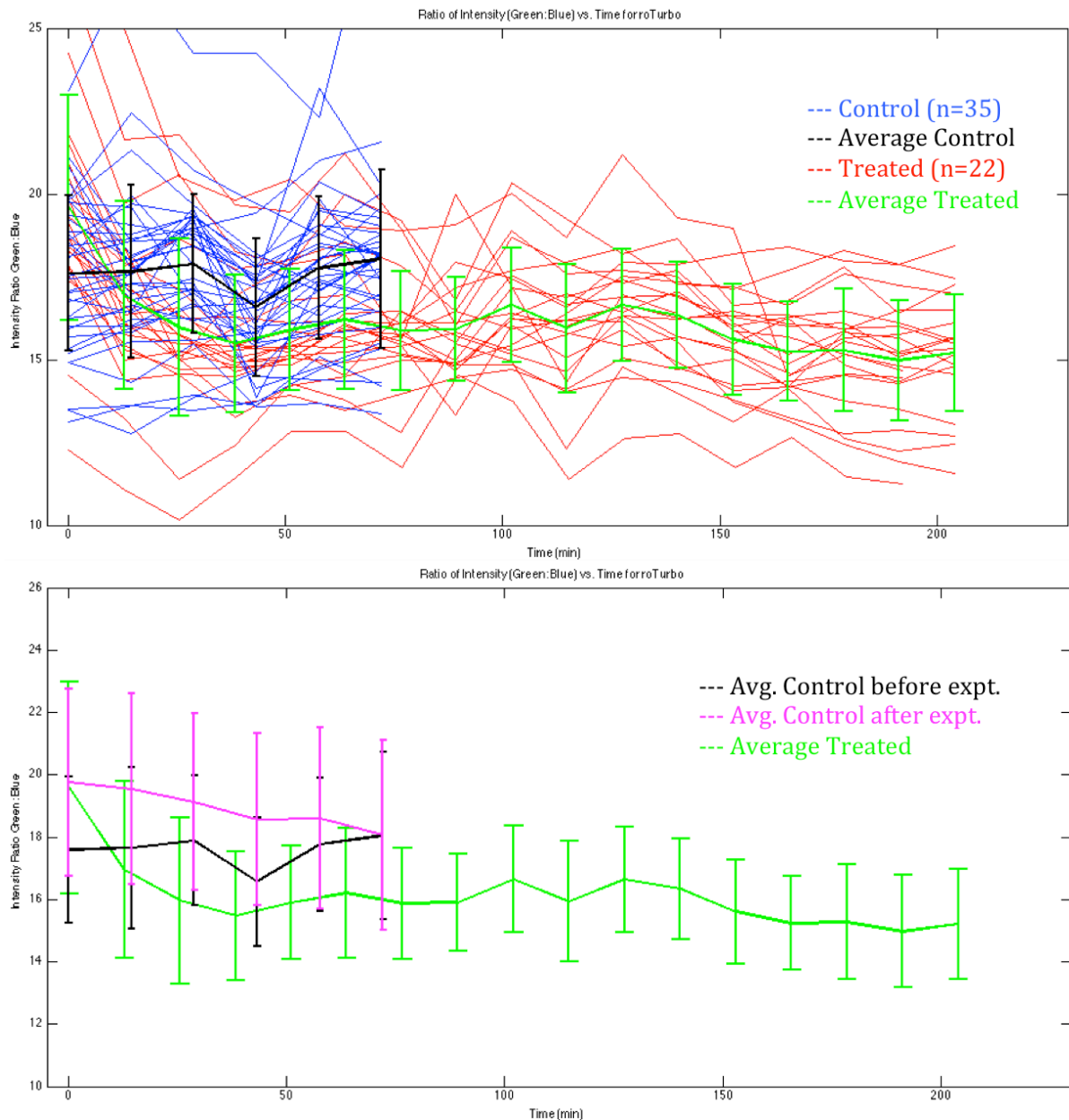**Figure 9: Live imaging with 250uM TBHP treatment (single replicate).** *Top Panel:* All 35 control N2a cells and 22 treated N2a cells for the 250uM TBHP overnight treatment. Control cells imaged only for one hour, treated cells died within 3.5 hours. *Bottom Panel:* Only the average plot of treated cells and control cells. Black line- control cells imaged prior to the TBHP treatment. Pink line- control cells

imaged after the overnight TBHP treatment (averaged over 26 cells). The pink line has been super-imposed starting from 0 minutes instead of at 720 minutes to give a better idea of relative values. All error bars represent standard error.
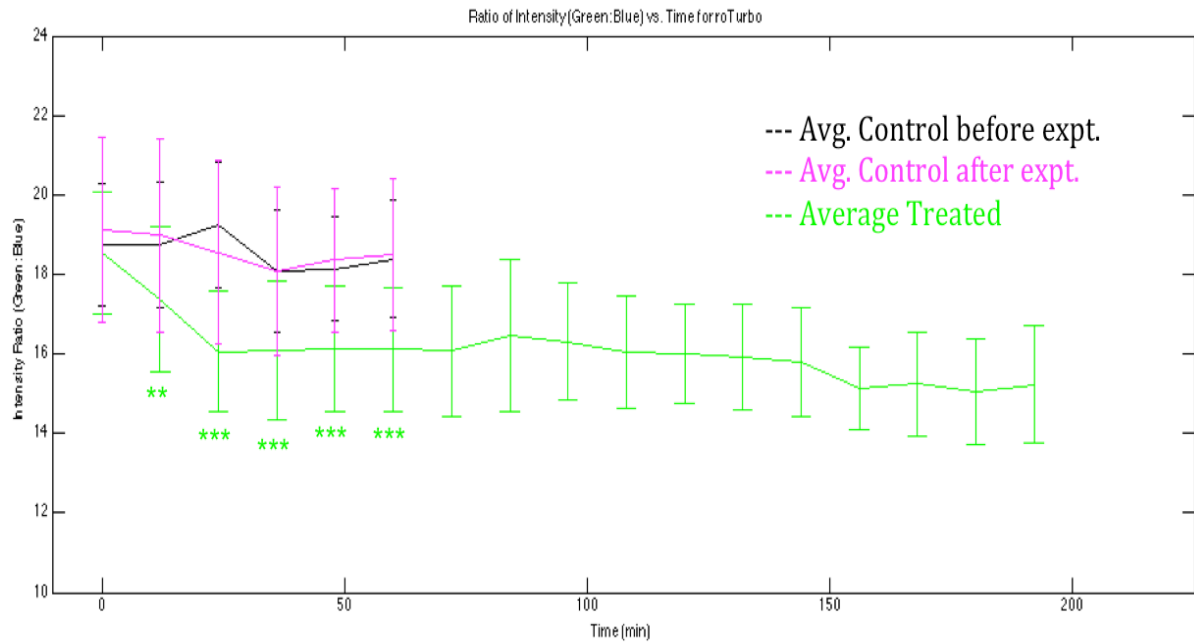
Figure 10: Live imaging with 250uM TBHP treatment (3 replicates). The average plots of treated N2a cells (n = 74 cells) and control N2a cells (n = 87 before expt. and n = 75 after expt.) from all three replicates pooled together for the 250uM TBHP overnight treatment. Control cells imaged only for one hour, treated cells died within 3.5 hours. Black line- control cells imaged prior to the TBHP treatment. Pink line- control cells imaged after the overnight TBHP treatment. The pink line has been super-imposed starting from 0 minutes instead of at 720 minutes to give a better idea of relative values. All error bars represent standard error.

Discussion

As we know, oxidative stress plays a major role in neurodegenerative disorders, and in order to study oxidative stress in real-time, we can use redox-sensing proteins. To this end, we successfully grew up the roGFP and roTurbo plasmids, cloned them into lentiviral backbones, and produced a roTurbo virus. We then monitored how cell lines would respond to an external oxidative stress producing agent- TBHP.

First, we performed some end-point experiments in order to gauge what concentrations of TBHP produce any effect on the cells, and what concentrations may prove to be extremely toxic to the cells (Figure 3). We observed that only 750uM and 1mM TBHP produced relevant effects on the cells. At 250uM and 500uM, we did not find a significant difference between treatment and control (in fact, the results seemed the opposite of what they should be- the treated cells seemed to have a higher ratio as compared to controls. However, due to large intercellular variability, these results were not significant). Although these results indicate to us what concentrations of TBHP we could use, one must realize that this is a mere starting place for the live imaging experiments. This is because end-point experiments do not give us sufficient insights into the nuances of the process. For instance, it could be possible that the lower concentrations of TBHP are also producing an effect on the cells, but the cells die out before the one-hour treatment is concluded. The surviving cells could be the ones that are immune to the treatment. Thus, while it might seem that the lower concentration of TBHP is not effective, it might be the case that the cells that where actually sensitive to the treatment are simply no longer present. Similarly, the data from the higher concentrations could also not include the cells that die earlier. Moreover, the experiment obviously cannot give a more subtle analysis of the change in oxidative stress over time. Thus, the end-point experiments only serve to give us initial clues as to what concentrations of TBHP we need to use for the live experiments.

Although we tried to perform the live-imaging experiments with transfected roGFP/roTurbo plasmids, the process of transfection led to persistent contamination over a few months. Thus, we decided to switch over to viral transduction, which

would only involve the addition of the virus, and no other reagents (unlike regular transfection), and would provide a stable expression. Moreover, the virus produced could also be used on primary neurons, as regular transfection is not effective on primary neurons. Therefore, we proceeded with the remainder of the experiments using lenti-roTurbo to transduce the cells.

We first tried the live imaging experiments on HEK293 cells, as they are more robust in terms of dealing with the external environment. Thus, our initial experiment involved imaging HEK cells with a 750uM overnight TBHP treatment (Figure 7). As can be seen, due to the large intercellular variability, it appears that there is no discernible pattern amongst the cells (Figure 7, Top Panel). However, a closer inspection of the results showed a different story. Around 30 or so cells that were treated showed an interesting trend, wherein the cells did indeed respond to the oxidative stress by a dip in the green:blue ratio, but then had a *rise* in the ratio after 15 minutes or so (Figure 7, Bottom Left panel). It could be the case though, that only one of the lasers (either blue or green) could be producing the trend, and hence the observed results could be caused due to some issue with the laser, and not an actual change in the intensity of the cells. Thus, in order to double check that it was indeed the result of the TBHP that the ratio was changing, we looked at the green intensities and the blue intensities separately (Figure 7, Bottom Right panels). We observed that not only was there a dip in the green intensity, but there was a rise in the blue intensity as well, thus ruling out problems with the laser.

Since the effect of adding 750uM TBHP was so quick (seen in only 10 minutes), we decided to repeat the experiment at a lower concentration of 500uM TBHP (Figure 8). As predicted, this time the effect is slower, lasting till about 30 minutes or so. Once again, we see the interesting feature of the green:blue ratio rising up, back to the levels seen in the control cells. One possible reason could be that the antioxidant mechanisms of the cell kick in after a critical point of oxidative stress is reached, and this helps the cell restore equilibrium once again. The lesser the concentration of TBHP, the longer it takes for the cell to reach the critical point of stress, hence the dip and the rise was seen at an earlier time point in 750uM TBHP as compared to 500uM. In the 500uM treated cells, there isn't as much variability as there was in 750uM TBHP, and the cells all seem to follow the same general pattern. The

intensity ratio of the control cells rises for a while, and then seems to plateau out, as can be seen in the flat ratio line for the control cells imaged after the TBHP treatment is done. Prior experiments utilizing roGFP or roTurbo just showed a drop in the green:blue ratio, eventually tapering off in an asymptote, and not the rebound. Although some studies do show a recovery phenomenon, this is usually when the oxidative stress-causing agent has been washed out (van Lith et al., 2011).

We then decided to move over to cells that would be closer to primary neurons- the neuroblastoma (N2a) cell line. Since this cell line is more sensitive to external conditions than HEK, we decided to drop the concentration of TBHP being used even lower, to 250uM (Figure 9, Figure 10). Here, we see a pronounced dip in the treated cells, but the recovery/rebound is nowhere near as good as that of the HEK293 cells. This could either be through the virtue of differences in the cell lines themselves, or because the concentration of TBHP used was not enough to help the cells attain the critical point of oxidative stress. Thus, the cells just seem to plateau out at the low green:blue ratio value. Further, there is more variability in the trend of the control cells as well. Once again, this is potentially due to the nature of the N2a cell line.

Future Directions

Thus, we see that the HEK and N2a cells respond to the addition of oxidative stress through a dip in the green:blue ratio, and a rebound (in case of HEK cells). The next step is to look at the how the oxidative state changes in the case of primary neurons harvested from the mouse cortex. Since we are looking at an Alzheimer's Disease model, we can look at the difference in the green:blue ratios for Wild Type neurons versus neurons from mice that are transgenic and express the APPswe/PS1ΔE9 mutation, thereby producing increased amounts of Aβ and hence having greater intrinsic oxidative stress. We would also like to look at the differences in the intensity ratios for the spines as compared to the neurite or the soma of the cells. This is especially interesting because there have been several studies to show that there are abnormalities seen in dendritic spines (Spires et al., 2005, Alpar et al., 2006),

neuronal breakage (Tsai et al., 2004), synapse loss and possibly spine loss as well in AD, and this is potentially due to increased Aβ levels. As Aβ is known to cause an increase in oxidative stress, a study along these lines should yield interesting results.

Furthermore, since the strength of the roGFP and roTurbo model is the real-time measurement of oxidative stress, rather than a static end-point measurement, we can also perform another experiment using a novel technique involving vanadium oxide (V_2O_5) nanowires. These nanowires play an anti-oxidant role, where they reduce the level of ROS within the cell (while leaving the cell unharmed) through a scavenging mechanism (Vernekar et al., 2014). Thus, we hope to see the real-time effects of oxidative stress in primary cortical neurons both when treated, and not treated with the V_2O_5 nanowires.

References

Alpar, A., Ueberham, U., Bruckner, M.K., Seeger, G., Arendt, T., Gartner, U. (2006). Different dendrite and dendritic spine alterations in basal and apical arbors in mutant human amyloid precursor protein transgenic mice. Brain Res *1099*,189–198.

Barnham, K.J., Masters, C.L., Bush A.I. (2004). Neurodegenerative diseases and oxidative stress. Nature Reviews *3*, 205-214.

Behl, C., Davis, J.B., Lesley, R., Schubert, D. (1994). Hydrogen Peroxide mediates Amyloid β protein toxicity. Cell *77*, 817-827.

Benzi, G., Pastoris, O., Marzatico, F., Villa, R.F., Dagani, F., Curti, D. (1992). The mitochondrial electron-transfer alteration as a factor involved in the brain aging. Neurobiol Aging *13*, 361–368.

Butler, J., Hoey, B.M. (1993). The one-electron reduction potential of several substrates can be related to their reduction rates by cytochrome-P-450 reductase. Biochim Biophys Acta *1161*, 73–78.

Chinta, S.J., Andersen, J.K. (2008). Redox imbalance in Parkinson's Disease. Biochim Biophys Acta, *1780*(11), 1362–1367.

Conway, K.A., Rochet, J.C., Bieganski, R.M., Lansbury, P.T. Jr. (2001). Kinetic stabilization of the alpha-synuclein protofibril by a dopamine-alpha-synuclein adduct. Science *294*, 1346-1349.

Damier, P., Hirsch, E.C., Agid, Y., Graybiel, A.M. (1999). The substantia nigra of the human brain II. Patterns of loss of dopamine-containing neurons in Parkinson's Disease. Brain *122*, 1437-1448.

Dias, V., Junn, E., Mouradian, M.M. (2013). The Role of Oxidative Stress in Parkinson's Disease. J Parkinsons Dis. *3*(4), 461–491.

Dizdaroglu, M., Jaruga, P., Birincioglu, M., Rodriguez, M. (2002). Free radical-induced damage to DNA: mechanisms and measurement. Free Rad. Biol. Med. *32*, 1102–1115.

Dooley, C.T., Dore, T.M., Hanson, G.T., Jackson, W.C., Remington, S.J., Tsien, R.Y. (2004). Imaging dynamic redox changes in mammalian cells with green fluorescent protein indicators. J Biol Chem. *279*, 22284–93.

Dooley, C.T., Li, L., Misler, J.A., Thompson, J.H. (2012). Toxicity of 6-hydroxydopamine: live cell imaging of cytoplasmic redox flux. Cell Biol Toxicol *28*, 89–101.

Emerit, J., Edeas, M., Bricaire, F. (2004). Neurodegenerative diseases and oxidative stress. Biomedicine & Pharmacotherapy *58*, 39-46.

Ermak, G., Davies, K.J.A. (2001). Calcium and oxidative stress: from cell signaling to cell death. Molecular Immunology *38*, 713-721.

Finkel, T., Holbrook, N.J. (2000). Oxidants, oxidative stress and the biology of ageing. Nature *408*, 239-247.

Freeman, A.B., Crapo, J.D. (1982). Free radicals and tissue injury. Biology of Disease *47*(5), 412-426

Goedert, M., Spillantini, M.G. (2006). A century of Alzheimer's Disease. Science *314*, 777-781.

Hanson, G.T., Aggeler, R., Oglesbee, D., Cannon, M., Capaldi, R.A., Tsien, R.Y., and Remington, S.J. (2004). J. Biol. Chem. *279*, 13044–13053.

Hwang, O. (2013). Role of Oxidative Stress in Parkinson's Disease. Experimental Neurobiology *22*(1), 11-17.

Inoue, M., Sato, E.F., Nishikawa, M., Park, A.M., Kira, Y., Imada, I., Utsumi, K. (2003) Mitochondrial generation of reactive oxygen species and its role in aerobic life, Curr. Med. Chem. *10*, 2495–2505.

Kadowaki, H., Nishitoh, H., Urano, F., et al. (2005). Amyloid β induces neuronal cell death through ROS-mediated ASK1 activation. Cell Death and Differentiation *12*, 19–24.

Kučera, O., Endlicher, R., Roušar, T., et al. The Effect of tert-Butyl Hydroperoxide-Induced Oxidative Stress on Lean and Steatotic Rat Hepatocytes In Vitro. Oxidative Medicine and Cellular Longevity, *2014*, Article ID 752506, 12 pages.

Lee, C.S., Han, J.H., Jang, Y.Y., Song, J.H., Han, E.S. (2002). Differential effect of catecholamines and MPP(+) on membrane permeability in brain mitochondria and cell viability in PC12 cells. Neurochem. Int. *40*, 361-369.

Li, F., Calingasan, Y.N., Yu, F., et al. (2004). Increased plaque burden in brains of APP mutant MnSOD heterozygous knockout mice. Journal of Neurochemistry *89*, 1308–1312.

Lloyd, R.V., Hanna, P.M., Mason, R.P. (1997). The origin of the hydroxyl radical oxygen in the Fenton reaction. Free Rad Biol Med *22*, 885–888

Loschen, G., Flohe, B. (1971). Chance respiratory chain linked H2O2 production in pigeon heart mitochondria, FEBS Lett. *18*, 261–263.

MathWorks (2011) MATLAB and Statistics Toolbox Release 2011b. The MathWorks, Inc., Natick, Massachusetts, United States.

McCord, J.M. (2000). The evolution of free radicals and oxidative stress. The American Journal of Medicine *108*, 652-659.

McKhann, G., Drachman, D., Folstein, M., Katzman, R., Price, D., and Stadlan, E.M. (1984). Clinical diagnosis of Alzheimer's disease. Neurology *34*, 939-944.

Miyata, M., Smith, J.D. (1996). Apolipoprotein E allele-specific antioxidant activity and effects on cytotoxicity by oxidative insults and beta-amyloid peptides. Nature Genetics *14*(1), 55-61.

Pedelacq, J.D., Cabantous, S., Tran, T., Terwilliger, T.C., Waldo, G.S. (2006). Engineering and characterization of a superfolder green fluorescent protein. Nat Biotechnol. *24*, 79–88.

Perry, G., Cash, A.D., Smith, M.A. (2002). Alzheimer Disease and Oxidative Stress. Journal of Biomedicine and Biotechnology *2*(3), 120-123.

Querfurth, H.W., LaFerla, F.M. (2010). Alzheimer's Disease. The New England Journal of Medicine 362, 329-44.

Smith, M.A., Richey Harris, P.L., Sayre, L., Perry, G. (1997). Iron accumulation in Alzheimer disease is a source of redox-generated free radicals. Proc. Natl. Acad. Sci. USA *94*, 9866–8.

Smith, M.A., Rottkamp, C.A., Nunomura, A., Raina, A.K., Perry, G. (2000). Oxidative stress in Alzheimer's disease. Biochimica et Biophysica Acta *1502*, 139-144.

Spires, T.L., Meyer-Luehmann, M., Stern, E.A., McLean, P.J., Skoch, J., Nguyen, P.T., Bacskai, B.J., Hyman, B.T. (2005). Dendritic spine abnormalities in amyloid precursor protein transgenic mice demonstrated by gene transfer and intravital multiphoton microscopy. Journal of Neuroscience *25*, 7278–7287.

Trelstad, R.L., Lawley, K.R., Holmes, L.B. (1981). Non-enzymatic hydroxylations of proline and lysine by reduced oxygen derivatives. Nature *289*, 310-2.

Tsai, J., Grutzendler, J., Duff, K., Gan, W.B. (2004). Fibrillar amyloid deposition leads to local synaptic abnormalities and breakage of neuronal branches. Nature Neuroscience *7*, 1181–1183.

Uttara, B., Singh, A.V., Zamboni, P., Mahajan, R.T. (2009). Oxidative stress and neurodegenerative diseases: A review of upstream and downstream antioxidant therapeutic options. Current Neuropharmacology *7*, 65-74.

Valko, M., Izakovic, M., Mazur, M., Rhodes, C.J., Telser, J. (2004). Role of oxygen radicals in DNA damage and cancer incidence. Mol. Cell. Biochem. *266*, 37–56

Valko, M., Rhodes, C.J., Moncola, J., Izakovic, M., Mazura, M. (2006). Free radicals, metals and antioxidants in oxidative stress-induced cancer. Chemico-Biological Interactions *160*, 1-40.

van Lith, M., Tiwari, S., Pediani, J., Milligan, G., Bulleid, N.J. (2011). Real-time monitoring of redox changes in the mammalian endoplasmic reticulum. Journal of Cell Science *124*, 2349-2356.

Vernekar, A.A., Sinha, D., Srivastava, S., Paramasivam, P.U., D'Silva, P., Mugesh, G. (2014). An antioxidant nanozyme that uncovers the cytoprotective potential of vanadia nanowires. Nature Communications *5*(5301), 1-13.

Wierer, S., Elgass, K., Bieker, S., Zentgraf, U., Meixner, A.J., Schleifenbaum, F. (2011). Determination of the in vivo redox potential using roGFP and fluorescence spectra obtained from one-wavelength excitation. Proc. SPIE *7902*, Imaging, Manipulation, and Analysis of Biomolecules, Cells, and Tissues IX, 790211.

Zecca, L., Wilms, H., Geick, S., et al. (2008). Human neuromelanin induces neuroinflammation and neurodegeneration in the rat substantia nigra: Implications for Parkinson's disease. Acta Neuropathol *116*, 47–55.

Zhao, Y., Zhao, B. (2013). Oxidative Stress and the Pathogenesis of Alzheimer's Disease. Oxidative Medicine and Cellular Longevity, Vol. *2013*, Article ID 316523.

Zhong, H., Yin, H. (2015). Role of lipid peroxidation derived 4-hydroxynonenal (4-HNE) in cancer: Focusing on mitochondria. Redox Biology *4*, 193-199.